

See discussions, stats, and author profiles for this publication at: <https://www.researchgate.net/publication/326725476>

Low-Energy Plasma Focus Proves Medical Grade Radioactivity Production

Article in IEEE Transactions on Plasma Science · July 2018

DOI: 10.1109/TPS.2018.2854920

CITATIONS

0

READS

45

4 authors, including:



Hossein Sadeghi

Amirkabir University of Technology

11 PUBLICATIONS 8 CITATIONS

[SEE PROFILE](#)



Samaneh Fazelpour

Amirkabir University of Technology

5 PUBLICATIONS 3 CITATIONS

[SEE PROFILE](#)



Sing Lee

INTI International University

407 PUBLICATIONS 4,685 CITATIONS

[SEE PROFILE](#)

Some of the authors of this publication are also working on these related projects:



Ion acceleration mechanism in PFD [View project](#)



Kansas State University Dense Plasma Focus [View project](#)

Low-Energy Plasma Focus Proves Medical Grade Radioactivity Production

M. V. Roshan¹, H. Sadeghi¹, S. Fazelpoor, and S. Lee

Abstract—The plasma focus (PF) emerged as a potential prospect to produce radionuclide, but the experimental data are not significant in favor of practical medical radioactivity. Empirical scaling grants a set of magnetic lens to enhance the nuclear activity. The experimental radioactivity of low-energy devices is in the range of kilobecquerel and rises to megabecquerel by optimizing and operating at a few hertz. Magnetically driven ion beam improves the radioactivity to the prescribed value of gigabecquerel for nuclear imaging. Magnetic radioactivity competence scheme reflects the vision that small PF, as a smart alternative to cyclotron, generates medical grade radioactivity.

Index Terms—Plasma Sources.

I. INTRODUCTION: NUCLEAR ACTIVITY DISCIPLINES IN PF

MOST of the experimental data on the nuclear activity production in the plasma focus (PF) have been reported on the solid targets, more specifically graphite, to produce ^{13}N radioactive nuclide. For gas targets, however, limited experimental data are available.

In the gas target experiments, chamber is filled with a mixture of gases constituting the target-projectile system. Gas mixture is composed of low-Z isotopes (hydrogen, deuterium, or helium) mixed with high-Z isotopes (nitrogen, oxygen, carbon dioxide, or air). Fast ions are trapped in magnetized plasma domains, and the nuclear reaction is induced by collisions with nuclei in the background plasma. Positron emitted from radioactive nuclei is measured by Geiger-Muller (GM) counter mounted inside the PF chamber. GM survives on electromagnetic shock and plasma jet. Seven-kilojoule PF operated in gas target experiments produces 100 kBq of ^{13}N through $^{12}\text{C}(d, n)^{13}\text{N}$ and 200 kBq ^{15}O through $^{14}\text{N}(d, n)^{15}\text{O}$ [1]. Identical PF at a different lab generated 37 kBq of ^{13}N and 20 kBq of ^{15}O [2]. The only difference between these two experiments was that β^+ was

Manuscript received January 27, 2018; revised May 22, 2018; accepted July 6, 2018. The review of this paper was arranged by Senior Editor J. L. Lopez. (Corresponding author: M. V. Roshan.)

M. V. Roshan is with the School of Particles and Accelerators, Institute for Research in Fundamental Sciences, IPM, Tehran 19395-5746, Iran (e-mail: mroshan20@yahoo.com).

H. Sadeghi is with the School of Particles and Accelerators, Institute for Research in Fundamental Sciences, IPM, Tehran 19395-5746, Iran, and also with the Physics Department, Amirkabir University of Technology, Tehran 15875-4413, Iran.

S. Fazelpoor is with the Physics Department, Amirkabir University of Technology, Tehran 15875-4413, Iran.

S. Lee is with Center for Plasma Research, INTI International University, Nilai 71800, Malaysia.

Color versions of one or more of the figures in this paper are available online at <http://ieeexplore.ieee.org>.

Digital Object Identifier 10.1109/TPS.2018.2854920

TABLE I

DIRECT AND SPECTRAL RADIOACTIVITY REPORTED FOR PF DEVICES

PF Discharge Energy (kJ)	Experimental Radioactivity (kBq)
76^{15}	160
57^{16}	86
20^{17}	28
10^4	23
6^{18}	4.88
5.4^{19}	4.35
5^{20}	4
4.7^{21}	3.73
2^{22}	1.45
$2^{14,3}$	5.6

measured inside the PF chamber in [1] and 511 keV γ from positron annihilation was measured outside the chamber in [2]. It was suggested that the reaction yield Y in plasma, gas target, is scaled with square of the energy stored in the capacitor bank: $Y \propto E^2$ [1].

In the solid target experiments, graphite is located on the forward PF axis at a typical distance of >10 cm from the pinch, and exposed to the accelerated deuterons [3]–[6]. The target was then removed from the PF chamber and placed in contact with a bismuth germanate scintillation detector. ^{13}N undergoes β^+ decay and 511 keV γ is produced by positron–electron annihilation process in the graphite target.

Predicted solid target nuclear activity with similar PF energy to that of gas target is 20 kBq of ^{13}N . If $Y \propto E^2$ for gas target is accepted, then the radioactivity generation in gas target would be higher than that in the solid target. However, the data on gas target radioactivity experiments are not sufficient and there are certain limitations for higher radioactivity production with this method.

One of the techniques to increase the radioactivity is to operate the device at high repetition rate. The NX2 device running at 1 kHz for 30 min generates an activity of 1 GBq [7]. It has been shown theoretically that if the time of PF operation is equal to the half-life of the particular radioisotope, then 10-Hz repetition rate with 10-kJ PF produces 50 mCi of ^{11}C and with 50-kJ PF produces 1 Ci of ^{18}F [1].

The maximum charge rate of the capacitors available today is 100 kJ/s (demands cooling system); hence, 1-MJ PF (with

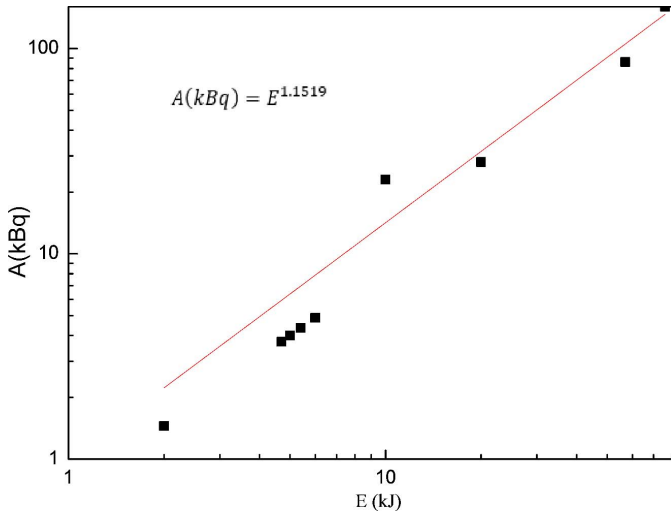


Fig. 1. Experimental radioactivity versus PF discharge energy.

massive charging system) takes 10 s to be fully charged. Furthermore, the pulsed power switches that can be operated at a few hertz with a peak current of about 400 kA in each discharge are not available. Besides, the capacitor bank for MJ device costs about U.S. \$480 000. Consequently, practical nuclear activity is constrained by limitations imposed by operating the device at higher repetition rate and energies. It follows that other methods need to be investigated to produce medical grade radioactivity in a PF device.

II. EXPERIMENTAL DATA AND OPTIMIZATION

Experimental data on the nuclear activity production in the PF (Table I) have been measured either directly or by using deuteron spectra. ^{13}N radioactivity A , per shot, as a function of PF discharge energy E fitted with power function

$$A(\text{kBq}) = E^{1.1519}(\text{kJ}) \quad (1)$$

is shown in Fig. 1. NX2 serves as a reference PF since accurate measurements on both direct and spectral activities have been reported on this device. It is a high repetition rate, up to 16 Hz [8], small Mather-type PF with 28- μF capacitor bank coupled to the PF electrodes through four pseudospark switches. The total system inductance is 26 nH, which is the optimum operating inductance of the device, providing the highest pinch current of 200 kA. The NX2 is operated with 4–14 mbar deuterium gas and 10–12-kV charging voltage. The plasma column is 2 mm in diameter and 10 mm in length, pinch duration of 70 ns, and temperature 0.5 keV. Direct measurement on NX2 gives 5.2 KBq [4] as an average radioactivity and at the best shot rises to 40 KBq [3]. The radioactivity calculated from the best deuteron spectrum shows 37 KBq for NX2.

The experimental data of Table I were optimized against NX2 radioactivity (Fig. 2) and fitted with power function of the form

$$A(\text{kBq}) = E^{1.4729}(\text{kJ}). \quad (2)$$

Nuclear activity estimation by the Lee model code [9] for some PF devices gives

$$A(\text{kBq}) = E^{1.04}(\text{kJ}) \quad (3)$$

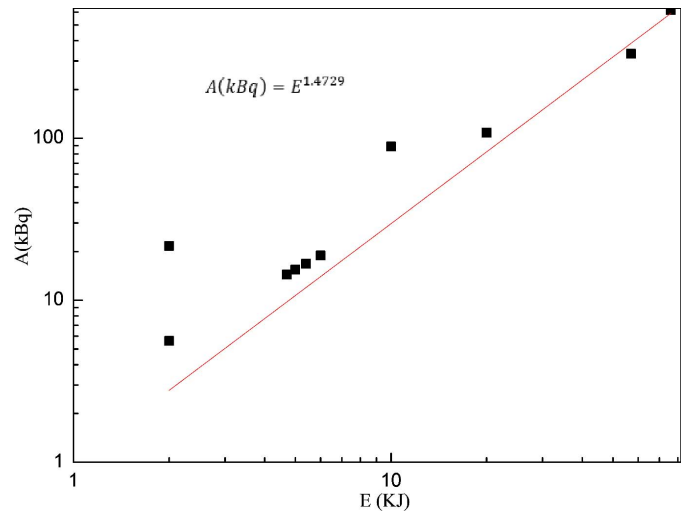


Fig. 2. Optimized radioactivity versus PF discharge energy.

TABLE II
EXPERIMENTAL, OPTIMIZED, AND LEE MODEL
RADIOACTIVITY FOR 1-MJ PF

<i>Predicted Experimental Data by Eq. 1</i>	<i>Optimized with NX2</i>	<i>Lee code</i>
7 MBq	22.4 MBq	1.5 MBq

which underestimates the real experimental data. For the most energetic PF device currently in operation, 1 MJ, the radioactivity predicted based on (1)–(3) is shown in Table II.

These estimations clearly show that the PF is far from being a suitable alternative to produce practical radioactivity. The best PF performance for maximum radioactivity is achieved in optimum pressure and voltage (operational features), and optimum inductance (design feature that increases the pinch current [10]). NX2 is the only device, among all presented in Table I, which has been designed to be operated at optimum inductance so that the highest radioactivity-to-energy ratio of $A/E \cong 3$ is obtained. It should also be pointed out that the experimental results could be fairly well compared in an identical context if the design and operational features are optimized for a PF.

III. MEDICAL GRADE NUCLEAR ACTIVITY

The maximum specific activity (SA) (Table III) for the common short-lived radionuclide (SLR) was estimated by: $SA = N_A \lambda (\text{Bq/mol})$, where λ is the decay constant and N_A is Avogadro's number. Table IV presents the deuteron-induced nuclear reaction in ^{12}C , ^{10}B , ^{14}N , and ^{20}Ne targets, corresponding Q -values (energy released) and threshold energy E_{th} (minimum energy of deuterons), and the minimum and maximum cross sections.

Substantial SA belongs to ^{15}O and the succeeding radionuclide is ^{13}N . Unlike that of solid target, experimental data on the gas target shows higher ^{15}O radioactivity compared to ^{13}N . The induced radioactivity in the solid target is

TABLE III
SA OF SLRs

Radionuclide	$\lambda(s^{-1})$	SA(Ci/ μ mol)	Radiation
^{18}F	1.05×10^{-4}	1710	97% β^+ 511 keV γ -ray
^{11}C	5.66×10^{-4}	2205	100% β^+ 511 keV γ -ray
^{13}N	1.16×10^{-3}	18853	100% β^+ 511 keV γ -ray
^{15}O	5.69×10^{-3}	92499	100% β^+ 511 keV γ -ray

TABLE IV
REACTION CROSS SECTION, Q -VALUE, AND THRESHOLD ENERGY FOR SLR PRODUCTION

Nuclear Reaction	Q -value (MeV)	E_{th} (MeV)	Deuterium Energy and cross section (minimum and maximum)	
$^{12}\text{C}(d,n)^{13}\text{N}$	-0.280	0.327	0.6 MeV: 10 mb	1.4 MeV: 130 mb
$^{10}\text{B}(d,n)^{11}\text{C}$	6.46	-7.76	4 MeV: 30 mb	7 MeV: 180 mb
$^{14}\text{N}(d,n)^{15}\text{O}$	5.07	-5.80	1.0 MeV: 10 mb	4.0 MeV: 210 mb
$^{20}\text{Ne}(d,\alpha)^{18}\text{F}$	2.79	-3.077	1.5 MeV: 10 mb	6.0 MeV: 220 mb

computed from

$$A = \frac{\lambda Y}{\varepsilon(1 - e^{-\lambda t_{\text{cnt}}})e^{-\lambda t_{\text{tr}}}} \quad (4)$$

where t_{cnt} is the counting time, t_{tr} is the transfer time (time between end of the activation and beginning of the count), ε is the efficiency of the detector, and Y is the reaction yield: $Y = N_d y_{\text{tt}}$ in which N_d is the total number of high-energy deuterons and y_{tt} is the tick target yield estimated to be 2.2×10^{-10} [11].

The bombardment time, set to be 600 s instead of being 60 s, improves the nuclear activity from 7% (5.2 kBq) to 50% (38 kBq) with the maximum feasible activity of about 77.5 kBq. Graphite activation by deuterons is the most favorable reaction since the minimum energy required is 0.6 MeV and the next reaction is ^{14}N activation to produce ^{15}O . In NX2, both ^{10}B and ^{14}N in a boron nitride solid target have been activated which reveals very high-energy deuterons of 4 MeV are exceptionally produced in a small 2-kJ PF device [6].

Reaction yield is proportional to the deuteron flux and, in a PF, flux turns out to be related to the pinch current [12] thus the radioactivity is

$$A = K I_p^2 y_{\text{tt}} (1 - e^{-\lambda t_b}) \quad (5)$$

where K is a constant reflecting the PF characteristics and I_p is the pinch current. Higher pinch current significantly

increases the radioactivity. Operating the PF at lowest possible inductance results in a greater pinch current.

The important parameters to be taken into account to maximize the radioactivity are as follows.

- 1) *Pinch Current*: Saturates at certain discharge energies [13].
- 2) *Deuteron Energy*: The spectrum configuration is identical for all PF devices, and drops exponentially at higher energies by a power of 7–9 [14].
- 3) *Bombardment Time*: Ultimately improves the radioactivity by one order of magnitude.
- 4) *Target Number Density*: For solid target is, typically, 10^{23} cm^{-3} , but for plasma domain (gas target) is 10^{21} cm^{-3} , and for the pinch is 10^{19} cm^{-3} .
- 5) *Cross Section*: Increases with energy.

Certain limitations exist in all five parameters above for maximum radioactivity production. However, it is shown that is possible to maximize the radioactivity to substitute the current bulky and expensive cyclotrons by a small, cheap, and simple PF device.

Most of the deuterons produced in the PF are moving in a cone with a half-angle of 25° against anode toward the upper part of the PF system with energy interval of a few electronvolts to several mega-electronvolts. The energy and number of ions depend on the PF discharge energy, leading to the point that the only parameter that can be optimized to significantly increase the radioactivity is to maximize the

TABLE V
MAGNETIC COIL SPECIFICATIONS

Coils No	Type	Radius (cm)	Current(A)	Number of turns
1	Coil	10	150	2000
2	Coil	8	150	2000
3	Copper Ring	9	0	1
4	Coil	8	150	2000
5	Coil	6.5	100	2000
6	Copper Ring	7.5	0	1
7	Coil	5.5	100	2000

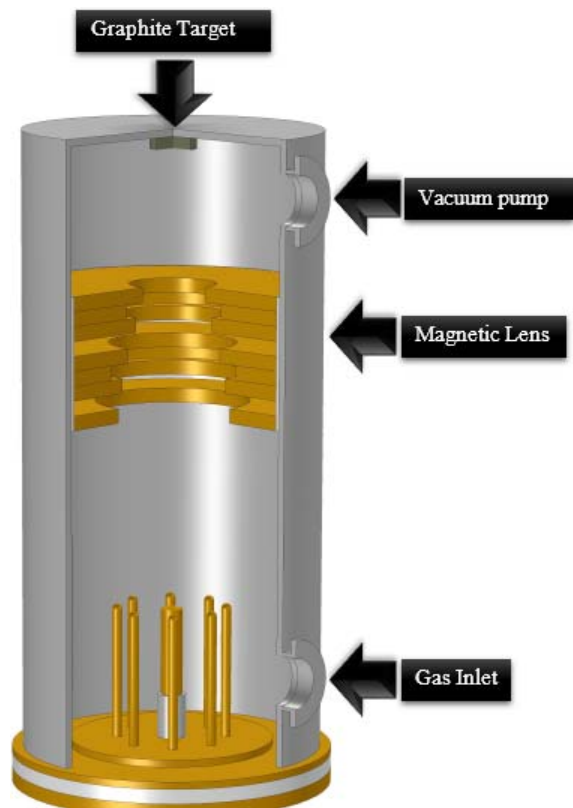


Fig. 3. Magnetic lens setup in the PF chamber.

fraction of ions interacting with target. One to two percent of ions generated in PF hit the target.

A set of magnetic lens with a particular configuration (Fig. 3) enables higher projectile-target collisions to enhance the radioactivity. The magnetic force within the PF device was examined by solving the equation of motion of a charged particle in a magnetic field. Strength of the lens depends upon the coil configuration and current. The charged particles are focused at a point along the z -axis. The focal length depends on the coil geometry and number of turns, the accelerating voltage, and the coil current. Energy of the charged particles increases the focal length since higher velocity reduces the time experiencing the magnetic field force. However, as the current increases so do the magnetic field strength, the charged particle gyrates in tighter paths bringing the focal length closer. This allows the focusing onto a surface in addition to adjusting the magnification.

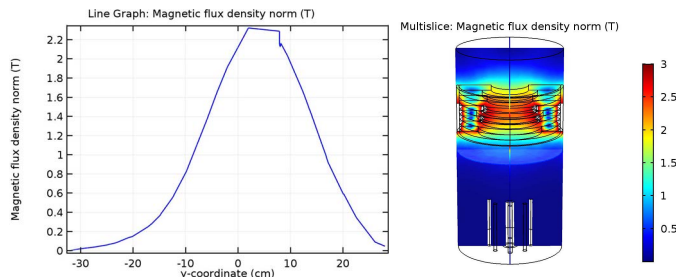


Fig. 4. Field configuration of the magnetic lens.

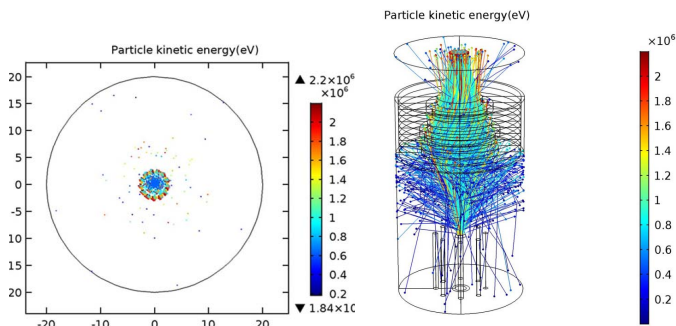


Fig. 5. Ion trajectory and localization cross section on the target by the magnetic lens.

The magnetic lens converges most of the ions $>90\%$ and focuses them on a small area on the target with a circular pattern of 2 cm in radius. The magnetic flux density of lens (Fig. 4) shows that the field on the anode head (-30 cm) is too small to influence the pinch formation and ion acceleration. The magnetic coil specifications are in Table V. COMSOL was used to design the magnetic lens and simulate the ion trajectory and localization on the target. Fast ions undergo interaction with neutral gas in the chamber; hence, the related parameters, such as elastic and inelastic scattering cross section, neutralization, and some other parameters, are considered for ion energy of 10 eV–10 MeV. Fig. 5 displays the ion trajectory and cross-sectional view of localized ion beam on the target.

The practical radioactivity for nuclear imaging, i.e., positron emission tomography, is 0.3–0.7 GBq. The maximum radioactivity, using magnetic lens, at 1- and 16-Hz repetition rate of PF discharges (Table VI) verifies that low-energy PF devices, such as NX2, PF10, and NX3, are potentially capable of generating medical grade activity. The radioactivity rises rapidly at lower PF energies and slows down at higher energies as shown in Fig. 6.

TABLE VI
MAGNETICALLY DRIVEN MAXIMUM RADIOACTIVITY

PF Device*	Discharge Energy (kJ)*	Ion No. (10^{14})*	Ion No. Entered Magnetic Lens (10^{12})	Radioactivity (kBq) one shot	Radioactivity (MBq) 16 Hz, 600 s
PF1000	486	6100	168.8	2480	17320
Poseidon	281	3300	86.4	1440	10000
Texas	126	1700	53.6	708	5000
PF115kJ	115.2	1771	56.58	760	5240
DPF78	31	390	12.6	180	1204
NX3	20	325	10.46	160	1000
PF11.5kJ	11.5	152	4.86	72	589
PF10kJ	10.6	104	3.29	48	334
PF5.4kJ	5.4	56	1.79	32	151
PF II	4.7	34.6	1.1	14.4	100
INTI	3.4	19	0.58	8.4	60
NX2	2.7	110	3.52	43.2	308
PF2.2	2.22	17.63	0.562	10	52
ICPT	2.16	15.4	0.482	8.8	48
PF5M	2	37	1.02	7.2	39
PF400J	0.4	5.9	0.12	2.4	16

*Data from Ref [9].

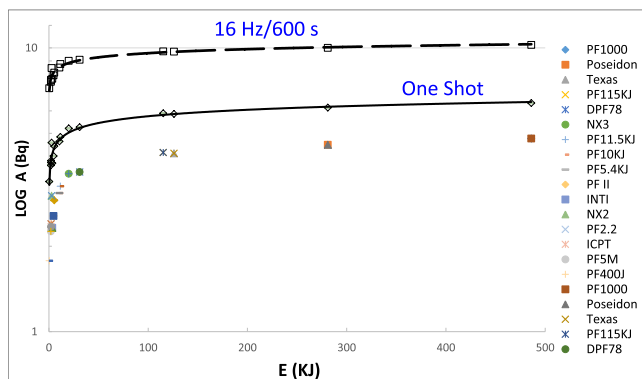


Fig. 6. Enhanced radioactivity at one shot and 16 Hz/600 s.

IV. CONCLUSION

The experimental data on the radioactivity production in the PF show an empirical scaling of the form $E^{1.1519}$. NX2 holds the highest radioactivity-to-energy ratio, and improves the scaling to $E^{1.4729}$. A set of magnetic lens intensifies the ion beam on a small area on the target and significantly promotes the radioactivity. Magnetically driven radioactivity of the NX2 is about 0.31 GBq. This confirms that the low-energy PF devices are the best alternatives to the cyclotrons for radionuclide production.

REFERENCES

- [1] J. S. Brzosko *et al.*, "Breeding 10^{10} /s radioactive nuclei in a compact plasma focus device," in *Proc. 16th AIP Int. Conf. Appl. Accel. Res. Ind.*, 2001, pp. 277–280.
- [2] E. Angeli *et al.*, "Production of radioisotopes within a plasma focus device," in *Proc. 5th Yugoslav Nucl. Soc. Conf.*, 2004, pp. 239–246.
- [3] M. V. Roshan, S. V. Springham, R. S. Rawat, and P. Lee, "Short-lived PET radioisotope production in a small plasma focus device," *IEEE Trans. Plasma Sci.*, vol. 38, no. 12, pp. 3393–3397, Dec. 2010.
- [4] M. V. Roshan *et al.*, "Potential medical applications of the plasma focus in the radioisotope production for PET imaging," *Phys. Lett. A*, vol. 378, pp. 2168–2170, Jun. 2014.
- [5] M. V. Roshan, S. V. Springham, A. R. Talebitaher, R. S. Rawat, and P. Lee, "Nuclear activation measurements of high energy deuterons from a small plasma focus," *Phys. Lett. A*, vol. 373, pp. 851–855, Feb. 2009.
- [6] M. V. Roshan, S. V. Springham, A. Rajasegaran, A. R. Talebitaher, R. S. Rawat, and P. Lee, "Intense deuteron beam investigation by activation yield-ratio technique," *Phys. Lett. A*, vol. 373, pp. 3771–3774, Oct. 2009.
- [7] M. Saed, M. V. Roshan, A. Banoushi, and M. Habibi, "The investigation capability of plasma focus device for ^{13}N radioisotope production by means of deuteron experimental spectrum," *J. Mod. Phys.*, vol. 7, no. 12, p. 1512, 2016.
- [8] S. Lee *et al.*, "High rep rate high performance plasma focus as a powerful radiation source," *IEEE Trans. Plasma Sci.*, vol. 26, no. 4, pp. 1119–1126, Aug. 1998.
- [9] M. Akel, S. A. Salo, S. Ismael, S. H. Saw, and S. Lee, "Interaction of the high energy deuterons with the graphite target in the plasma focus devices based on Lee model," *Phys. Plasmas*, vol. 21, no. 7, p. 072507, 2014.
- [10] F. Karami, M. V. Roshan, M. Habibi, P. Lee, S. H. Saw, and S. Lee, "Neutron yield scaling with inductance in plasma focus," *IEEE Trans. Plasma Sci.*, vol. 43, no. 7, pp. 2155–2159, Jul. 2015.
- [11] M. V. Roshan, R. S. Rawat, A. Talebitaher, R. Verma, P. Lee, and S. V. Springham, "High energy deuteron emission in NX2 plasma focus," *J. Plasma Fusion Res. SERIES*, vol. 8, pp. 1273–1276, Dec. 2009.
- [12] S. Lee and S. H. Saw, "Plasma focus ion beam fluence and flux—For various gases," *Phys. Plasmas*, vol. 20, no. 6, p. 062702, 2013.
- [13] V. Y. Nukulin and S. N. Polukhin, "Saturation of the neutron yield from megajoule plasma focus facilities," *Plasma Phys. Rep.*, 33, no. 4, pp. 271–277, 2007.

- [14] M. V. Roshan, S. V. Springham, A. Talebitaher, R. S. Rawat, and P. Lee, "Magnetic spectrometry of high energy deuteron beams from pulsed plasma system," *Plasma Phys. Controlled Fusion*, vol. 52, no. 8, p. 085007, 2010.
- [15] W. Stygar, G. Gerdin, F. Venneri, and J. Mandrekas, "Particle beams generated by a 6–12.5 kJ dense plasma focus," *Nucl. Fusion*, vol. 22, no. 9, p. 1161, 1982.
- [16] A. Mozer, M. Sadowski, H. Herold, and H. Schmidt, "Experimental studies of fast deuterons, impurity- and admixture-ions emitted from a plasma focus," *J. Appl. Phys.*, vol. 53, no. 4, pp. 2959–2964, 1982.
- [17] B. Bienkowska, S. Jednorog, I. M. Ivanova-Stanik, M. Scholz, and A. Szydowski, "Application of the ion beam emitted from plasma focus device for target activation," *Acta Phys. Slovaca*, vol. 54, no. 4, pp. 401–407, 2004.
- [18] L. Rapezzi *et al.*, "Development of a mobile and repetitive plasma focus," *Plasma Sources Sci. Technol.*, vol. 13, no. 2, p. 272, 2004.
- [19] W. H. Bostick, H. Kilic, V. Nardi, and C. W. Powell, "Time resolved energy spectrum of the axial ion beam generated in plasma focus discharges," *Nucl. Fusion*, vol. 33, no. 3, p. 413, Mar. 1993.
- [20] V. Nardi and C. Powell, "The plasma focus as a source of collimated beams of negative ion clusters and of neutral deuterium atoms," in *Proc. AIP Conf.*, vol. 111, 1984, pp. 463–472.
- [21] M. Sadowski, A. Szydowski, M. Scholz, H. Kelly, A. Marquez, and A. Lepone, "Application of solid-state nuclear track detectors for studies of fast ion beams within PF-1000 and other plasma-focus facilities," *Radiat. Meas.*, vol. 31, pp. 185–190, Jun. 1999.
- [22] M. Sadowski *et al.*, "Comparison of characteristics of pulsed ion beams emitted from different small PF devices," *Nukleonika*, vol. 45, no. 3, pp. 179–184, 2000.

Authors' photographs and biographies not available at the time of publication.